Direct Enantioseparation of Lorlatinib Enantiomers by Liquid Chromatography on a Chiralpak IB Column

[1]Mengya Liao, [2]Xin Wang, [3]Qin Wang* and [2]Yiwen Zhang

[1]*Center of Gerontology and Geriatrics, West China Hospital, Sichuan University, Chengdu 610041, China.*

[2]*Cancer Center, West China Hospital, Sichuan University, Chengdu 610041, China.*

[3]*Department of Endocrinology and Metabolism, West China Hospital, Sichuan University, Chengdu 610041, China.*

wq3166@163.com*

(Received on 20th May 2022, accepted in revised form 30th September 2022)

Summary: Enantiomeric forms of many drugs are known to have different physiological and therapeutic effects. Previous studies indicated that the inhibitory activity of an enantiomer of Lorlatinib on L1196M kinase was 300 times lower than that of Lorlatinib. In this study, an analytical method for the enantioseparation of Lorlatinib was established on a Chiralpak IB column. Baseline separation was obtained within 10 min using *v*(*n*-hexane): *v*(2-propanol): *v*(diethylamine) = 85:15:0.1 as mobile phase, and a resolution higher than 2.2. Various factors of HPLC such as the effect of chiral columns, the contents of mobile phase and column temperature were thoroughly investigated. Calibration curves were plotted within the concentration range between 10 and 1000 μg mL^{-1} (*n* = 8), and recoveries between 97.86% and 100.99% were obtained, with a relative standard deviation (RSD) lower than 1.6%. The LOD and LOQ for Lorlatinib were 10.34 and 34.49 μg mL^{-1}, respectively, and those for its enantiomer were 11.76 and 39.21 μg mL^{-1}, respectively. Validating factors such as the accuracy, precision, linear relationship, and LOD/LOQ confirmed that the method has the advantages of high efficiency, accuracy and stability and can be used to detect the enantiomeric purity of Lorlatinib. In addition, the chiral recognition mechanisms were discussed according to the thermodynamic parameters and simulation studies between racemates and CSPs.

Keywords: NSCLC; Lorlatinib; Chiral separation; Enantiomeric purity.

Introduction

Classification of lung cancer

The mortality rate of lung cancer is highest among all malignant tumors worldwide. Lung cancer is divided into small-cell lung cancer (SCLC) and non-small-cell lung cancer (NSCLC) according to the type of incidence. NSCLC accounts for the vast majority of the two types of lung cancer (generally more than 80%). Lung adenocarcinoma (LUAD, 50%) and lung squamous cell carcinoma (LSCC, 30%) are the most common types of NSCLC. Large cell lung cancer (LCLC) also belongs to the NSCLC category (accounting for 2-3%), and it is the third most common clinicopathological type of NSCLC [1, 2].

Characteristics and treatment of patients with NSCLC

In recent decades, the average survival time of patients diagnosed with NSCLC has been less than 6 months. A recent epidemiological survey of lung cancer found that younger people tended to develop lung cancer, and lung cancer was the most common lethal tumor in both men and women. Even if lung cancer is found and diagnosed early, the current traditional medical treatment mode cannot improve the prognosis of patients [3, 4].

The treatment methods for NSCLC include surgery, radiotherapy, chemotherapy, targeted therapy, and biological immunotherapy. The specific treatment plan depends on the pathology and stage of the disease, the presence or absence of mutant genes, the toxicity and side effects during treatment, and the wishes and conditions of the patient. With the development of tumor molecular biology, a large number of key genes of signaling pathways related to the occurrence, development and metastasis of lung cancer have been identified and deeply studied. An increasing number of genes have been widely studied, and may be targets for the diagnosis and treatment of NSCLC. A large number of drugs that target tumor-specific targets have emerged, and most of these drugs are monoclonal antibodies and small molecular compounds [5, 6].

EML4-ALK and ROS1

EML4-ALK was first discovered in 2007,

*To whom all correspondence should be addressed.

and it was confirmed to be a lung cancer driver gene. The EML4-ALK fusion gene accounts for approximately 3-5% of NSCLC cases, and it is an important target in NSCLC. The EML4-ALK fusion gene has a high incidence in young NSCLC patients, nonsmokers, light smokers, and adenocarcinoma carriers without EGFR gene mutations. In recent years, a variety of drugs that target anaplastic lymphoma kinase tyrosine kinases (ALK-TKIs) have been sequentially approved to market, which has greatly changed the clinical treatment mode of patients with ALK-positive NSCLC [7].

The ROS1 fusion gene is a type of driving NSCLC gene subtype with relatively low frequency. Research indicated that ROS1 and ALK have 77% homology in the ATP binding site of the kinase catalytic region. Therefore, ALK-TKI inhibitors can also be used to treat patients with ROS1 gene-positive NSCLC. However, similar to other TKI inhibitors, patients will acquire drug resistance to ALK-TKI within 1-2 years [7].

ALK-TKI inhibitors

Because ALK is rarely expressed in normal adult tissues, targeted therapy with ALK-TKI inhibitors has relatively low toxicity and few side effects in the treatment of ALK-positive NSCLC, which has become the mainstream treatment for ALK-positive NSCLC.

Crizotinib, a first-generation ALK-TKI inhibitor, was used as a first-line treatment of patients with advanced ALK-positive NSCLC [8]. Brigatinib, Alectinib, and Ceritinib are efficient, highly selective and oral effective second-generation ALK-TKI inhibitors. According to their sensitivity to different secondary drug-resistant mutations of ALK, appropriate second-generation ALK-TKI inhibitors can be selected for the treatment of patients with Crizotinib resistance [9, 10]. Lorlatinib, also known as PF-06463922, is the first third-generation of ALK inhibitor, and is an orally available ATP-competitive selective inhibitor of receptor tyrosine kinases, ALK and ROS1 [11, 12]. In 2005, Pfizer developed Lorlatinib as a drug against NSCLC [13]. Previous studies have shown that first- and second-generation ALK-TKI inhibitors are not sensitive to G1202R-resistant mutations, while Lorlatinib has high selectivity and good antitumor activity against almost all ALK-resistant mutations including G1202R. Lorlatinib has high CNS permeability and good anti-intracranial tumor activity in patients with ALK-positive brain metastasis NSCLC. Pfizer's clinical data showed that among patients with brain metastases with ALK rearrangement, the ORR of Lorlatinib reached 31%. At present, Lorlatinib is widely used as a first-line drug for the treatment of NSCLC [14-18].

HPLC and CSPs

High-performance liquid chromatography (HPLC) is the backbone of separation science, as it is being used in almost all industries, including the pharmaceutical, chemical, and agro- or food-processing industries. Therefore, HPLC methods need to be developed for rapid analyses, especially in the pharmaceutical, biological and environmental sciences. Currently, worldwide economic pressure demands that HPLC analyses be fast and efficient [19-21].

The chiral methyl group is very important for the conformational stability of Lorlatinib. Previous studies indicated that the inhibitory activity of its enantiomer on L1196M kinase was 300 times lower than that of Lorlatinib. According to FDA regulations, drugs with enantiomers should be separated to obtain single configuration compounds for related research [22]. Therefore, the determination of the enantiomeric purity of Lorlatinib is very important. A large number of experimental studies have shown that chiral resolution can be easily obtained using high performance liquid chromatography (HPLC) combined with chiral stationary phases (CSPs) [23, 24]. Among the existing commercial CSPs, polysaccharide CSPs are considered to be one of the most effective CSPs for analysis or preparation chromatography. Polysaccharide CSPs mainly include cellulose and amylose. Their raw materials are inexpensive and easy to obtain. They are polymers with optical activity formed by glucose units that exist in nature. This type of CSP has a wide range of chiral recognition and a large amount of loading. According to the data statistics, more than 90% of HPLC chiral separation procedures were carried out on this type of CSP [25, 26].

According to the preparation methods, polysaccharide CSPs can be divided into coated and immobilized CSPs. By using aminopropylated macroporous silica gel as a carrier, the coated CSPs are prepared by coating polysaccharide derivatives on the surface of macroporous silica gel. At present, many types of coated polysaccharide commercial

columns are available on the market. However, coated polysaccharide CSPs also have fatal disadvantages. The polysaccharide derivatives are connected with macroporous silica gel by physical adsorbent, with only intermolecular interactions. Organic solvents, such as tetrahydrofuran, acetonitrile and chloroform, will dissolve and wash away the polysaccharide derivatives. Therefore, coated CSPs cannot be used in the reverse-phase system, which limits the application of coated CSPs to a great extent. Compared with coated CSPs, bonded CSPs have several obvious advantages, such as higher stability and the use of any mutually soluble as the mobile phase and the solvent for dissolving the sample. Since the use of solvent is unlimited, the dissolution of the coated filler of the chiral column due to the improper use of solvent, which may in damage to the chiral column, is not a concern. At present, bonded CSPs are developing rapidly, and many of them have been commercialized.

In the preparation of polysaccharide CSPs, to obtain more selective chiral recognizers, the hydroxyl groups on cellulose or amylose are usually derivatized, and then coated or bonded on carriers such as macroporous silica gel to prepare the corresponding CSPs. When chiral recognition is carried out, the derivative groups on the chiral selector such as the amino group, carbonyl group, benzene ring, and substituents on the benzene ring can have dipole-dipole interactions, hydrogen bond interactions and pi-pi interaction with the enantiomer. At the same time, the helical structure of cellulose or amylose and the steric effect produced by chiral holes can form diastereomeric complexes with different stabilities between the enantiomer and the stationary phase. Thus, the enantiomers can be separated under elution of the mobile phase on polysaccharide CSPs.

In previous research, liquid chromatography-tandem mass spectrometry and RP-HPLC have been used for the identification of Lorlatinib in mouse plasma and in tablet dosage form, respectively [27, 28]. At present, efforts to obtain chiral resolution of Lorlatinib enantiomers have never been reported. Therefore, an efficient and low-cost method needed to be developed to separate Lorlatinib enantiomers. The aim of this work was to develop a rapid and precise LC method to determine the enantiomeric purity of Lorlatinib. In this research, five different representative polysaccharide chiral columns were used for separation.

Experimental

Chemicals

Lorlatinib (*R*-enantiomer) was purchased from Med Chem Express (Shanghai, China). The racemate sample was synthetized according to Johnson *et al*. [7] (the synthetic route is shown in Fig. 1). Ethanol, 2-propanol and *n*-hexane of LC grade were purchased from Fisher (Suwanee, GA, USA). High purity water was produced by a Milli-Q gradient A10 water purification system (Millipore, Molsheim, France) and used for all experiments. The raw materials for the synthesis of racemates (such as 2-amino-3-hydroxypyridine, 1*H*-pyrazole-5-carbonitrile, 1-(5-fluoro-2-iodophenyl)ethenone, 4-bromo-1,3-dimethyl-1*H*-pyrazole-5-carboxylic acid methyl ester, etc) and other reagents of analytical grade were purchased from Kelong Chemical Co., Ltd. (Chengdu, China).

Instrumentation

The HPLC system was a Waters Alliance system separation module e2695 (Waters Corporation, Massachusetts, USA), consisting of a binary pump, column oven and autoinjector coupled with a Waters 2998 PDA detector. The output signals and analytical data were collected and processed by the Empower 3® software (Waters Corporation, Massachusetts, USA). Columns of Chiralpak AD-H, Chiralcel OD-H, Chiralpak IA, Chiralpak IB and Chiralpak IC (250×4.6 mm; particle size 5 μm; Daicel, Osaka, Japan) were tested for separation. Chromatographic parameters such as retention time, retention factor, and peak areas, were calculated using the Empower 3® software.

Chromatographic Conditions

Five different types of chiral stationary phases (CSPs), as mentioned above, were used for the experiment. *n*-Hexane and 2-propanol/ethanol were used as the mobile phase, and the column temperature was set to 30 °C. The flow rate was 1 mL min^{-1}, and the diode array detector (DAD) was set to 260 nm. The void time was measured by using ethyl acetate as a marker. The injection volume was 20 μL. The sample solutions were prepared by dissolving the samples in 2-propanol.

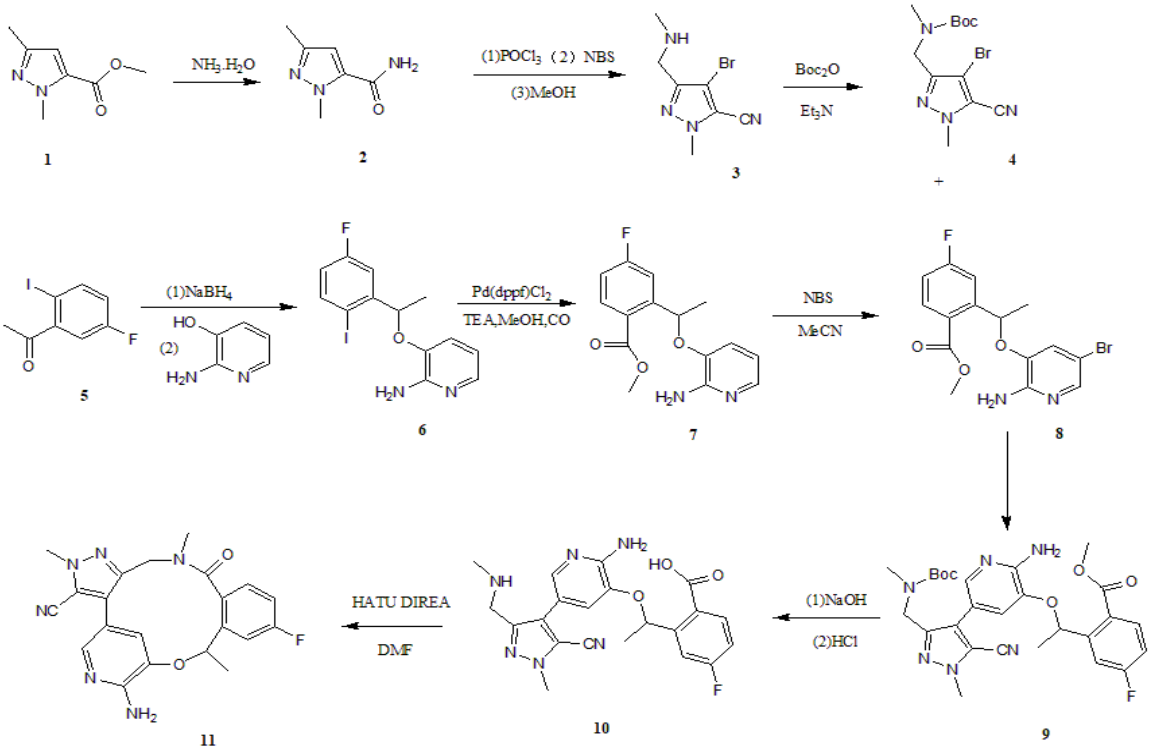

Fig. 1: Synthetic route of racemate sample.

Plasma sample preparation

Plasma samples were prepared as reported by Fang *et al* [29]. After rats received a single intravenous dose of Lorlatinib (40 mg kg^{-1}), the amount Lorlatinib in the plasma was determined by the method established above. Blood samples (2.0 mL) were collected from rats at the designated time point (30 min). All rats remained conscious throughout the sample collection period. The samples were chilled and immediately centrifuged at 3500 rpm for 10 min to obtain the plasma. The supernatant was transferred into another glass tube and evaporated to dryness under a gentle stream of nitrogen at 37 °C. The residue was reconstituted with the mobile phase and vortexed for 1 min. The samples were frozen and preserved at -20 °C until analysis.

Simulation Studies

The modeling was performed with a high-performance computing workstation (28 core, 56 thread processor, 64 GB memory), Accelrys Discovery Studio (v3.1) software package, ChemOffice 2014 and other molecular simulation software. The molecular structure of the Lorlatinib enantiomers was drawn using Chem Bio Draw 14.0.0.117 in the Chem office 2014 software package. The three-dimensional conformations of Lorlatinib enantiomers were generated using the Accelrys Discovery Studio (v3.1) software package, and energy minimization was carried out to retain the molecular conformation with energy minimization. Moreover, CHARMm with energy parameters was also used for energy minimization. The optimal conformations of CSP and the interaction between the two enantiomers were simulated by Accelrys Discovery Studio (v3.1). In this study, the calculated binding energies module (MMGBSA dG Bind) was used to calculate the binding energy of the complex between enantiomer and CSP.

Results and Discussion

Preparation of the racemate sample

According to the synthetic procedure, the racemate sample of Lorlatinib was obtained. The spectral data of the products in each step are described below.

Compound 2: ^{1}H NMR (400 MHz, DMSO-d_6): δ 7.78 (s, 1H), 7.37 (s, 1H), 6.59 (s, 1H), 3.96 (s, 3H), 2.12 (s, 3H). HRMS $[M+H]^+$ calculated for 140.07,

found 140.03.

Compound 3: ^{1}H NMR (400 MHz, DMSO-d_6): δ 3.90 (s, 2H), 3.78 (s, 3H), 2.48 (s, 3H), 2.02 (s, 1H). HRMS $[M+H]^+$ calculated for 329.05, found 329.01.

Compound 4: ^{1}H NMR (400 MHz, DMSO-d_6): δ 4.41 (d, 2H), 4.03 (s, 3H), 2.87 (s, 3H), 1.37-1.48 (s, 9H). HRMS $[M+H]^+$ calculated for 407.41, found 407.23.

Compound 6: ^{1}H NMR (400 MHz, $CDCl_3$): δ 7.37 (dd, 1H), 7.61 (dd, 1H), 7.09 (dd, 1H), 6.73 (ddd, 1H), 6.53-6.42 (m, 2H), 5.42-5.31 (m, 1H), 4.76 (s, 2H), 1.64 (d, 3H). HRMS $[M+H]^+$ calculated for 359.01, found 359.03.

Compound 7: ^{1}H NMR (400 MHz, $CDCl_3$): δ 8.06 (dd, 1H), 7.58 (dd, 1H), 7.24 (dd, 1H), 6.98 (ddd, 1H), 6.59 (dd, 1H), 6.40 (dd, 1H), 6.29 (q, 1H), 4.73 (s, 2H), 3.96 (s, 3H), 1.63 (d, 3H). HRMS $[M+H]^+$ calculated for 291.11, found 291.07.

Compound 8: ^{1}H NMR (400 MHz, $CDCl_3$): δ 8.08 (dd, 1H), 7.69 (dd, 1H), 7.27 (dd, 1H), 7.06 (ddd, 1H), 6.77 (d, 1H), 6.36 (q, 1H), 4.85-4.77 (s, 2H), 3.99 (s, 3H), 1.67 (d, 3H). HRMS $[M+H]^+$ calculated for 369.02, found 369.08.

Compound 9: ^{1}H NMR (400 MHz, $CDCl_3$): δ 8.05 (m, 1H), 7.67 (s, 1H), 7.28 (dd, 1H), 7.02 (m, 1H), 6.71 (m, 1H), 6.42 (m, 1H), 4.92 (s, 2H), 4.33-4.24 (m, 2H), 3.98 (s, 3H), 3.92 (s, 3H), 2.87-2.58 (m, 3H), 1.71 (d, 3H), 1.27 (s, 9H). HRMS $[M+H]^+$ calculated for 539.23, found 539.19.

Compound 10: ^{1}H NMR (400 MHz, CD_3OD): δ 8.09 (dd, 1H), 7.54 (d, 1H), 7.45 (dd, 1H), 7.26 (d, 1H), 7.18 (dt, 1H), 6.75 (dd, 1H), 4.26 (d, 1H), 4.18 (d, 1H), 4.11 (s, 3H), 2.78 (s, 3H), 1.79 (d, 3H). HRMS $[M+H]^+$ calculated for 425.17 found 425.12.

Compound 11: ^{1}H NMR (400 MHz, DMSO-d_6): δ 7.58-7.52 (m, 2H), 7.43 (dd, 1H), 7.16 (t, 1H), 6.77 (s, 1H), 6.17 (s, 2H), 5.57 (m, 1H), 4.42-4.38 (dd, 1H), 4.17-4.14 (dd, 1H), 4.00 (s, 3H), 2.95 (s, 3H), 1.65 (d, 3H). HRMS $[M+H]^+$ calculated for 407.41, found 407.23. $C_{21}H_{19}FN_6O_2$: measured (calculated), %: C 62.03 (62.06), H 4.75 (4.71), F 4.63 (4.67), N 20.71 (20.68), O 7.89 (7.87).

Choice of chiral stationary phases

To optimize the optimal separation conditions of the enantiomers, two different mobile phases (2-propanol in *n*-hexane and ethanol in *n*-hexane) were tested using five previously mentioned commercial chiral columns, which showed that only the Chiralpak IB column could completely separate the enantiomers of Lorlatinib. Furthermore, by using Chiralpak IB, other parameters were further investigated to obtain the optimal conditions.

Effect of Organic Modifier

The types and proportions of the organic modifier are the most indispensable factors that affect the resolution of enantiomers. The results are shown in Table-1, and better separation behavior was obtained with 2-propanol. Moreover, the baseline separation of the racemate could be improved by adding 0.1% diethylamine to the mobile phase. Increasing of the proportion of organic modifier decreased the interaction between the sample and the stationary phase. Thus, a 85:15 ratio of 0.1% diethylamine to *n*-hexane–2-propanol was used as the optimal mobile phase for the resolution of Lorlatinib enantiomers. The chromatogram of the optimal conditions is shown in Fig. 2.

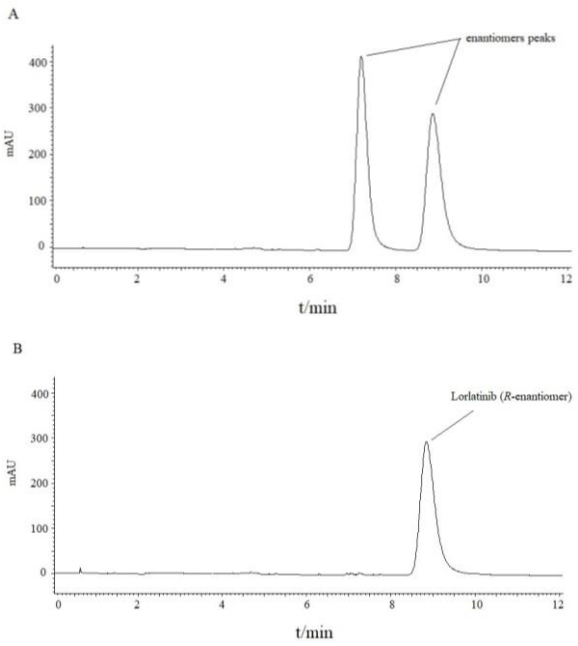

Fig. 2: Chromatograms for racemate on Chiralpak IB.
Chromatographic conditions: mobile phase: *n*-hexane: 2-propanol: diethylamine (85:15:0.1, *v/v/v*); column temperature: 30 ˚C; flow rate: 1.0 mL min^{-1}; UV detection wavelength: 260 nm.
Samples concentration: (A): racemate, 0.8 mg mL^{-1}; (B): Lorlatinib, 0.4 mg mL^{-1}.

Table-1: The influence of the composition of mobile phase on the seperation efficiency.

Mobile phase	k_1	k_2	t_1	t_2	α	R_S
Hex:EtOH =90:10	2.62	3.38	11.23	13.59	1.29	1.33
Hex:EtOH =85:15	2.03	2.63	9.42	11.28	1.30	1.21
Hex:EtOH:DEA =85:15:0.1	1.07	1.43	6.43	7.55	1.34	1.38
Hex:IPA = 90:10	3.71	4.85	14.62	18.15	1.31	1.62
Hex:IPA = 85:15	3.05	3.91	12.57	15.24	1.28	1.38
Hex:IPA:DEA =90:10:0.1	1.74	2.49	8.49	10.83	1.43	2.58
Hex:IPA:DEA = 85:15:0.1	1.34	1.85	7.27	8.86	1.38	2.21
Hex:IPA:DEA = 80:20:0.1	0.90	1.24	5.89	6.94	1.37	1.76

Hex: *n*-hexane; IPA: 2-propanol; EtOH: ethanol; DEA: diethylamine; k_1: retention factor of Lorlatinib's enantiomer (*S*-enantiomer); k_2: retention factor of Lorlatinib; t_1: retention time of Lorlatinib's enantiomer (*S*-enantiomer); t_2: retention time of Lorlatinib; α: separation factor; R_s: resolution; stationary phase: Chiralpak IB; flow rate: 1.0 mL min^{-1}; column temperature: 30 ˚C; UV detection wavelength: 260 nm.

Effect of Temperature

Temperature is an important factor affecting resolution [30-35]. The effect of column temperature within the range of 293-308 K (20-35 ˚C) on the chiral resolution of the Loratinib enantiomers was investigated, and the results are shown in Table-2. The retention time and retention factor decreased with the increasing temperature, and the results of the thermodynamic study were consistent with the Van't Hoff equations. This finding indicates that the interaction between the sample and CSPs decreases with increasing temperature.

Table-2: Thermodynamic data for Lorlatinib enantiomers.

Parameters	*S*-enantiomer	Lorlatinib
Slope	1085.5	1027.6
Intercept	-3.28	-2.77
R^2	0.995	0.993
ΔH^θ / (kJ mol^{-1})	-9.025	-8.544
$\Delta\Delta H^\theta$ / (kJ mol^{-1})	0.481	
ΔS^θ / (J $K^{-1}mol^{-1}$)	-27.28	-22.99
$\Delta\Delta S^\theta$ / (J $K^{-1}mol^{-1}$)	4.29	
$\Delta\Delta G^\theta$ / (kJ mol^{-1})	-1.757 (303K)	

Method Validation

(1) *Linearity and LOD/LOQ*

The calibration curves were obtained with freshly prepared solutions of Lorlatinib and its enantiomer in the concentration range of 10 to 1000 μg mL^{-1} (n = 8) with r_1^2= 0.9992 and r_2^2=0.9994 and the regression equations were y_1=6239.5x_1-49780 and y_2=6265.6x_1-58702, respectively. Different concentrations of Lorlatinib enantiomers were prepared until the signal-to-noise ratio (peak height/baseline noise) was 3±1 as the LOD and 10±2 as the LOQ. The respective LOD and LOQ were found to be 10.34 and 34.49 μg mL^{-1} for Lorlatinib and 11.76 and 39.21 μg mL^{-1} for its enantiomers.

(2) *Enantiomeric purity*

The enantiomeric purity is an important parameter in the production of pharmaceutical products of acceptable quality. The mobile phase was optimized to discriminate Lorlatinib from its chiral impurity (*S*-isomer). To assess the method's ability to separate the chiral impurities from the active isomers, the prepared pure Lorlatinib isomers were spiked with its corresponding racemic mixture at the 1%, 2% and 5% levels of the main peak. The method was optimized to achieve sufficient resolution and detect the *S*-isomer at low levels of the main peak by spiking the pure 100 μg mL^{-1} Lorlatinib using the prepared racemic solutions of each (1.0, 2.0 and 5.0 μg mL^{-1} of the racemic solution). As shown in Fig. 3, no interference from the chiral impurity was observed at the 1% level of the main peak. The developed method was found to be efficient for the determination of the enantiomeric purity of Lorlatinib in pharmaceutical preparation. Good resolution between isomers, high detector sensitivity and baseline stability were essential to detect trace amounts of *S*-isomer at a level of (1%) of the main peak.

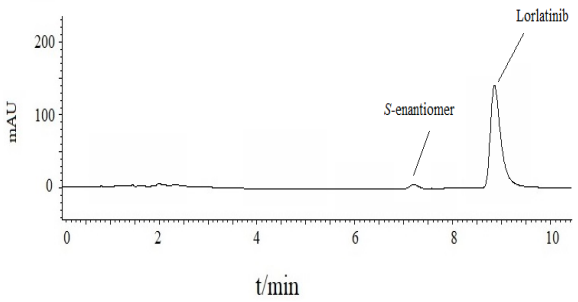

Fig. 3: Enantiomeric purity testing of Lorlatinib done by spiking 100 μg mL^{-1} with its corresponding racemic mixture of concentration 1.0 μg mL^{-1} (1% ratio).

(3) *Accuracy*

The experiment was carried out by testing three concentrations (50, 200, 500 μg mL^{-1}) of Lorlatinib enantiomer solutions. The recovery of all enantiomers was 97.86%~100.99% with RSD% not exceeding 1.6% (Table-3).

Table-3: Accuracy experiment for the Lorlatinib enantiomers.

Concentration (μg mL^{-1})		Found (μg mL^{-1})	RSD (%)	Recovery (%)
S-enantiomer	50	49.46	0.9	98.92
	200	198.47	1.4	99.23
	500	502.96	1.2	100.59
Lorlatinib	50	48.93	1.6	97.86
	200	201.57	0.8	100.78
	500	504.97	1.3	100.99

(4) *Precision*

Three concentrations (50, 200, 500 μg mL^{-1}) of the Lorlatinib enantiomers were used for the precision experiment. The RSD of retention time and peak area were 0.01%~0.76% and 0.02%~0.68%, respectively, and the results indicated that the accuracy of the method was good.

(5) *Robustness*

Under optimal chromatographic conditions, the robustness of the analytical method was investigated by changing various parameters, such as the column temperature, flow rate and 2-propanol ratio. According to the experimental results in Table-4, the slight changes in chromatographic conditions did not affect the separation of the Lorlatinib enantiomers.

Determination of enantiomeric purity of Lorlatinib in plasma

Fig. 4 shows that this method can be used to determine the enantiomeric purity of Lorlatinib in plasma. Moreover, this method can be applied for drug analysis in plasma.

Assay of Bulk Drugs

Three samples of different enantiomeric purities of lorlatinib were prepared with racemate: Lorlatinib at ratios of 1:9, 1:4 and 4:1. The RSD% did not exceed 1.6% (Table-5).

Table-4: Robustness for method

Variable parameter	Modifcation	*Rs*
IPA (%)	14.5	2.23
	15	2.21
	15.5	2.18
Temperature (°C)	28	2.24
	30	2.21
	32	2.19
flow rate (mL min^{-1})	0.9	2.25
	1.0	2.21
	1.1	2.18

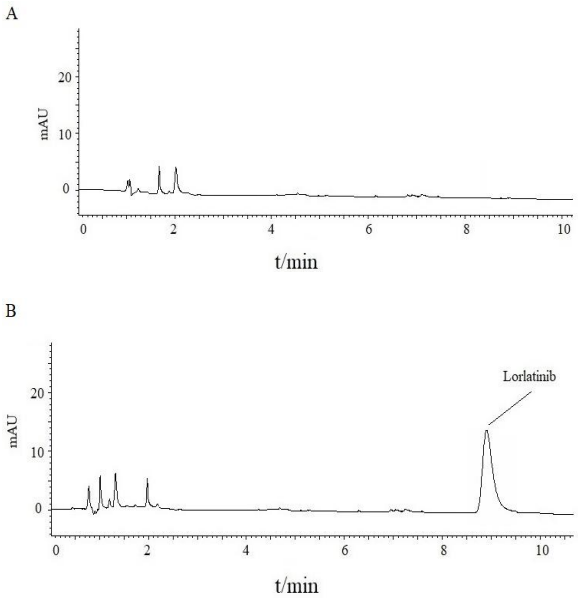

Fig. 4: (A) a blank chromatogram for plasma, (B) Chromatograms of Lorlatinib enantiomers in plasma.
Chromatographic conditions: mobile phase: *n*-hexane: 2-propanol: diethylamine (85:15:0.1, *v/v/v*); column temperature: 30 °C; flow rate: 1.0 mL min^{-1}; UV detection wavelength: 260 nm.

Table-5: Lorlatinib in real samples.

Serial number	Lorlatinib (%)	RSD (%)	Minor enantiomer	RSD (%)
1	94.48	1.43	5.57	1.68
2	89.72	1.51	10.63	1.34
3	59.69	1.58	40.41	1.71
4	49.82	1.39	50.42	1.46

4 was racemate.

Chiral Recognition Mechanism

The chiral recognition mechanism was studied by simulation software calculation. The MMGBSA of Lorlatinib and the *S*-enantiomer were calculated to be -45.82 and -39.07 kJ mol^{-1}, respectively. The calculation results revealed that the MMGBSA was negative for all analytes, which is consistent with the previous experimental results. The interaction between the racemate and CSPs is shown in Fig. 4. As shown in Fig. 5, two pi-pi interactions and two hydrogen bonds were observed between Lorlatinib and CSPs, and two pi-pi interactions and one hydrogen bond were observed between the *S*-enantiomer and CSPs.

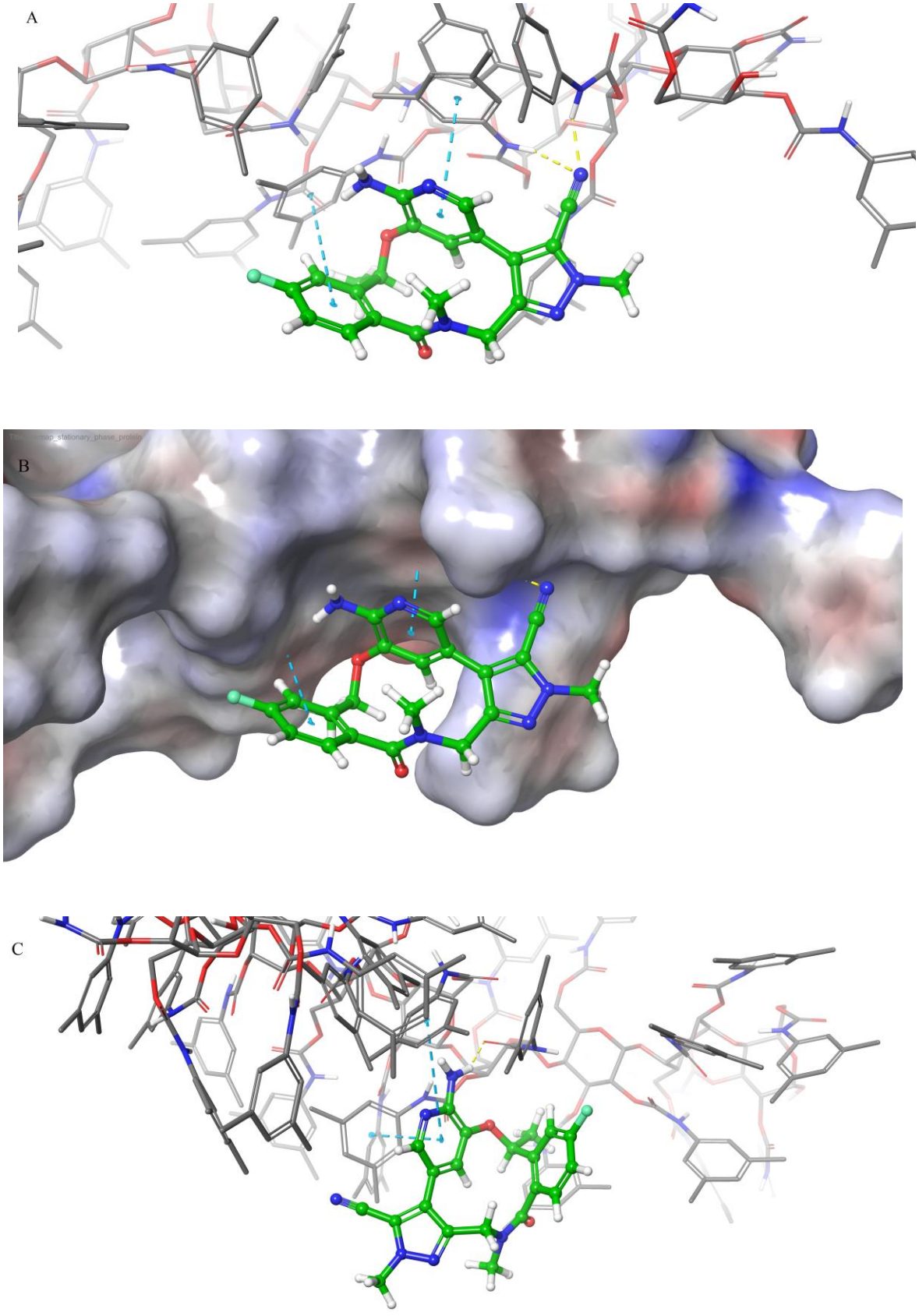
A
B
C

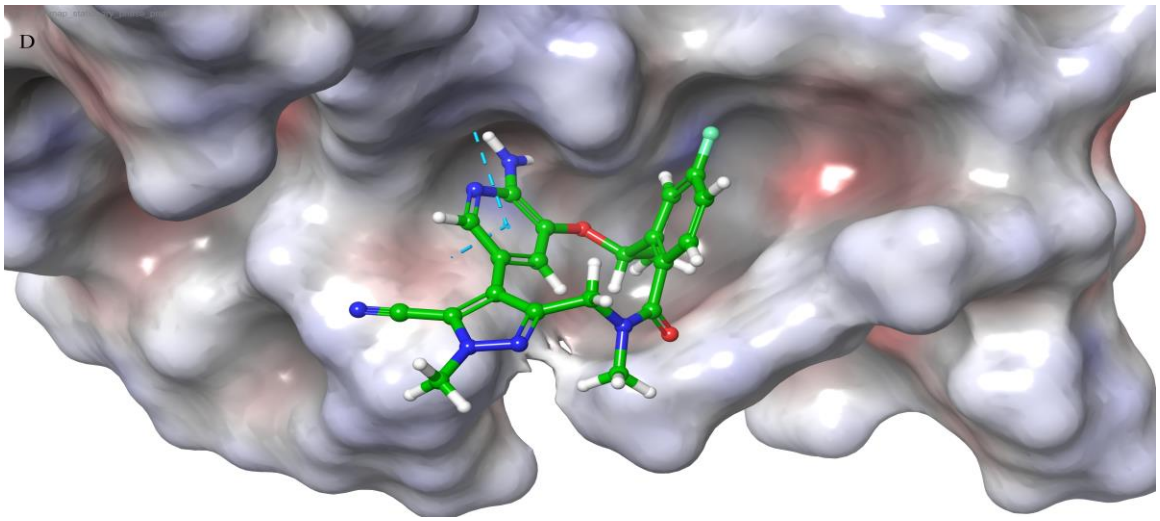

Fig. 5: The interaction between the racemate and CSPs. (A-B): Lorlatinib; (C-D) *S*-enantiomer. Blue dotted lines indicate pi-pi interactions, and yellow dotted lines indicate hydrogen bond.

Conclusions

The enantioseparation of Lorlatinib was achieved on a Chiralpak IB column, and the this separation was optimized with the use of *n*-hexane: 2-propanol: diethylamine (85:15:0.1, *v/v*) as the mobile phase, at a column temperature of 30 $^{\circ}$C and a flow rate of 1.0 mL min^{-1}. At this condition, the resolution of enantiomers was >2.2, and the analytical time was less than 10 min, which meets the requirements of rapid analysis. This chiral-HPLC method can provide an accurate and reliable analytical method for the separation and quantitative determination of the enantiomeric purity of Lorlatinib.

Funding

This study was funded by the Support Program of Science & Technology Department of Sichuan Provincial (No. 2021YFH0173) and Chengdu Science and Technology Bureau International cooperation projects (No. 2019-GH02-00036-HZ).

References

1. S. Pedersen, K. P. Jensen, B. Honoré, S. R. Kristensen, C. H. Pedersen, W. M. Szejniuk, R. G. Maltesen and U. Falkmer, Circulating microvesicles and exosomes in small cell lung cancer by quantitative proteomics, *Clin. Proteomics*, **19**, 2 (2022).
2. N. Heersche, G. D. M. Veerman, M. de With, S. Bins, Y. G. Assaraf, A. C. Dingemans, R. H. N. van Schaik, R. H. J. Mathijssen and F. G. A. Jansman, Clinical implications of germline variations for treatment outcome and drug resistance for small molecule kinase inhibitors in patients with non-small cell lung cancer, *Drug Resist. Updat.*, **62**, 100832 (2022).
3. R. Zaim, K. Redekop, C. A. U. Groot, Analysis of patient reported outcomes included in the registrational clinical trials of nivolumab for advanced non-small cell lung cancer, *Transl. Oncol.*, **20**, 101418 (2022).
4. J. Sun, S. Wu, Z. Jin, S. Ren, W. C. Cho, C. Zhu and J. Shen, Lymph node micrometastasis in non-small cell lung cancer, *Biomed. Pharmacother.*, **149**, 112817 (2022).
5. J. Hou, H. Li, S. Ma, Z. He, S. Yang, L. Hao, H. Zhou, Z. Zhang, J. Han, L. Wang and Q. Wang, EGFR exon 20 insertion mutations in advanced non-small-cell lung cancer: current status and perspectives, *Biomark Res.*, **10**, 21 (2022).
6. X. Zheng, J. Luo, W. Liu, C. R. Ashby Jr, Z. Chen and L. Lin, Sotorasib: a treatment for non-small cell lung cancer with the KRAS G12C mutation, *Drug. Today*, **58**, 175 (2022).
7. S. Basit, Z. Ashraf, K. Lee and M. Latif, First macrocyclic 3rd-generation ALK inhibitor for treatment of ALK/ROS1 cancer: Clinical and designing strategy update of lorlatinib, *Eur. J. Med. Chem.*, **134**, 348 (2017).
8. S. Ignatius Ou, E. L. Kwak, C. Siwak-Tapp, J. Dy, K. Bergethon, J. W. Clark, D. R. Camidge, B. J. Solomon, R. G. Maki, Y. Bang, D. Kim, J. Christensen, W. Tan, K. D. Wilner, R. Salgia and A. J. Iafrate, Activity of crizotinib

(PF02341066), a dual mesenchymal-epithelial transition (MET) and anaplastic lymphoma kinase (ALK) inhibitor, in a non-small cell lung cancer patient with de novo MET amplification, *J. Thorac. Oncol.*, **6,** 942 (2011).

9. L. Friboulet, N. Li, R. Katayama, C. C. Lee, J. F. Gainor, A. S. Crystal, P. Michellys, M. M. Awad, N. Yanagitani, S. Kim, A. C. Pferdekamper, J. Li, S. Kasibhatla, F. Sun, X. Sun, S. Hua, P. McNamara, S. Mahmood, E. L. Lockerman, N. Fujita, M. Nishio, J. L. Harris, A. T. Shaw and J. A. Engelman, The ALK inhibitor ceritinib overcomes crizotinib resistance in non-small cell lung cancer, *Cancer Discov.*, **4**, 662 (2014).
10. R. Katayama, L. Friboulet, S. Koike, E. L. Lockerman, T. M. Khan, J. F. Gainor, A. J. Iafrate, K. Takeuchi, M. Taiji, Y. Okuno, N. Fujita, J. A. Engelman and A. T. Shaw, Two novel ALK mutations mediate acquired resistance to the next-generation ALK inhibitor alectinib, *Clin. Cancer Res.*, **20**, 5686 (2014).
11. T. W. Johnson, P. F. Richardson, S. Bailey, A. Brooun, B. J. Burke, M. R. Collins, J. J. Cui, J. G. Deal, Y. L. Deng, D. Dinh, L. D. Engstrom, M. He, J. Hoffman, R. L. Hoffman, Q. Huang, R. S. Kania, J. C. Kath, H. Lam, J. L. Lam, P. T. Le, L. Lingardo, W. Liu, M. McTigue, C. L. Palmer, N. W. Sach, T. Smeal, G. L. Smith, A. E. Stewart, S. Timofeevski, H. Zhu, J. Zhu, H. Y. Zou and M. P. Edwards, Discovery of (10*R*)-7-amino-12-fluoro-2,10,16-trimethyl-15-oxo-10,15,16,17-tetrahydro-2*H*-8,4-(metheno)pyrazolo[4,3-*h*][2,5,11]-benzoxadiazacyclotetradecine-3-carbonitrile (PF-06463922), a macrocyclic inhibitor of anaplastic lymphoma kinase (ALK) and c-ros oncogene 1 (ROS1) with preclinical brain exposure and broad-spectrum potency against ALK-resistant mutations, *J. Med. Chem.*, **57**, 4720 (2014).
12. H. Y. Zou, Q. Li, L. D. Engstrom, M. West, V. Appleman, K. A. Wong, M. McTigue, Y. L. Deng, W. Liu, A. Brooun, S. Timofeevski, S. R. P. McDonnell, P. Jiang, M. D. Falk, P. B. Lappin, T. Affolter, T. Nichols, W. Hu, J. Lam, T. W. Johnson, T. Smeal, A. Charest and V. R. Fantin, PF-06463922 is a potent and selective next-generation ROS1/ALK inhibitor capable of blocking crizotinib-resistant ROS1 mutations, *P. Natl. Acad. Sci. USA*, **112**, 3493 (2015).
13. H. Y. Zou, L. Friboulet, D. P. Kodack, L. D. Engstrom, Q. Li, M. West, R. W. Tang, H. Wang, K. Tsaparikos, J. Wang, S. Timofeevski, R. Katayama, D. M. Dinh, H. Lam, J. L. Lam, S. Yamazaki, W. Hu, B. Patel, D. Bezwada, R. L. Frias, E. Lifshits, S. Mahmood, J. F. Gainor, T. Affolter, P. B Lappin, H. Gukasyan, N. Lee, S. Deng, R. K. Jain, T. W. Johnson, A. T. Shaw, V. R. Fantin and T. Smeal, PF-06463922, an ALK/ROS1 Inhibitor, Overcomes Resistance to First and Second Generation ALK Inhibitors in Preclinical Models, *Cancer Cell*, **28**, 70 (2015).
14. R. Roskoski Jr, Anaplastic lymphoma kinase (ALK) inhibitors in the treatment of ALK-driven lung cancers, *Pharmacol. Res.*, **117**, 343 (2017).
15. J. F. Gainor, L. Dardaei, S. Yoda, L. Friboulet, I. Leshchiner, R. Katayama, I. Dagogo-Jack, S. Gadgeel, K. Schultz, M. Singh, E. Chin, M. Parks, D. Lee, R. H. DiCecca, E. Lockerman, T. Huynh, J. Logan, L. L. Ritterhouse, L. P. Le, A. Muniappan, S. Digumarthy, C. Channick, C. Keyes, G. Getz, D. Dias-Santagata, R. S. Heist, J. Lennerz, L. V. Sequist, C. H. Benes, A. John. Iafrate, M. Mino-Kenudson, J. A. Engelman and A. T. Shaw, Molecular Mechanisms of Resistance to First- and Second-Generation ALK Inhibitors in ALK-Rearranged Lung Cancer, *Cancer Discov.*, **6**, 1118 (2016).
16. A. T. Shaw, E. Felip, T. M. Bauer, B. Besse, A. Navarro, S. Postel-Vinay, J. F. Gainor, M. Johnson, J. Dietrich, L. P. James, J. S. Clancy, J. Chen, J. Martini, A. Abbattista and B. J. Solomon, Lorlatinib in non-small-cell lung cancer with ALK or ROS1 rearrangement: an international, multicentre, open-label, single-arm first-in-man phase 1 trial, *Lancet Oncol.*, **18**, 1590 (2017).
17. S. N. Waqar and D. Morgensztern, Lorlatinib: a new-generation drug for ALK-positive NSCLC, *Lancet Oncol.*, **19**, 1555 (2018).
18. J. Guan, E. R. Tucker, H. Wan, D. Chand, L. S. Danielson, K. Ruuth, A. El Wakil, B. Witek, Y. Jamin, G. Umapathy, S. P. Robinson, T. W. Johnson, T. Smeal, T. Martinsson, L. Chesler, R. H. Palmer and B. Hallberg, The ALK inhibitor PF-06463922 is effective as a single agent in neuroblastoma driven by expression of ALK and MYCN, *Dis. Model. Mech.*, **9**, 941 (2016).
19. I. Ali, Z. A. Al-Othman, N. Nagae, V. D. Gaitonde and K. K. Dutta, Recent trends in ultra-fast HPLC: new generation superficially porous silica columns, *J. Sep. Sci.*, **35**, 3235 (2012).
20. I. Ali, Z. A. Al-Othman and M. Al-Za'abi, Superficially porous particles columns for super-fast HPLC separations, *Biomed. Chromatogr.*, **26**, 2001 (2012).
21. I. Ali, V. D. Gaitonde and H. Y. Aboul-Enein,

Monolithic silica stationary phases in liquid chromatography, *J. Chromatogr. Sci.*, **47**, 432 (2009).
22. No authors listed, FDA's policy statement for the development of new stereoisomeric drugs, *Chirality*, **4**, 338 (1992).
23. Z. Afzal, N. Rashid and H. Nadeem, Stereoselective Synthesis, Spectral Characterization, Docking and Biological Screening of Coumarin Derivatives, *J. Chem. Soc. Pakistan*, **43**, 330 (2021).
24. D. C. Wang, C. Wu, C. Zhang, F. Z. Zhou, H. Song and X. P. Liu, Efficient Construction of 4-hydroxy-4-arylbutan-2-ones through an Enantioselective Aldol Reaction Mediated by a Recoverable Proline-Based Chiral Ionic Liquid, *J. Chem. Soc. Pakistan*, **42**, 243 (2020).
25. X. Wang, H. Li, K. Quan, L. Zhao, H. Qiu and Z. Li, Preparation and applications of cellulose-functionalized chiral stationary phases: A review, *Talanta*, **225**, 121987 (2021).
26. G. D'Orazio, M. Asensio-Ramos and C. Fanali. Enantiomers separation by capillary electrochromatography using polysaccharide-based stationary phases, *J. Sep. Sci.*, **42**, 360 (2019).
27. C. Spatari, W. Li, A. H. Schinkel, G. Ragno, J. H. M. Schellens, J. H. Beijnen and R. W. Sparidans. Bioanalytical assay for the quantification of the ALK inhibitor lorlatinib in mouse plasma using liquid chromatography-tandem mass spectrometry, *J. Chromatogr. B*, **1083**, 204 (2018).
28. N. D. Anuradha and A. N. Syed. RP-HPLC method development and validation for the determination of Lorlatinib in bulk and its pharmaceutical formulation, *World J. Pharm. Pharm. Sci.*, **8**, 1142 (2019).
29. A. Fang, Y. Zhang, J. Shen, S. Sun, J. Zou and Y. Yao. Determination of AR-42 enantiomeric purity by HPLC on chiral stationary phase, *J. Iran. Chem. Soc.*, **14**, 1909 (2017).
30. Q. Sun and S. V. Olesik, Chiral separation by simultaneous use of vancomycin as stationary phase chiral selector and chiral mobile phase additive, *J. Chromatogr. B Biomed. Sci. Appl.*, **745**, 159 (2000).
31. G. S. Ding, Y. Liu, R. Z. Cong and J. D. Wang, Chiral separation of enantiomers of amino acid derivatives by high-performance liquid chromatography on a norvancomycin-bonded chiral stationary phase, *Talanta*, **62**, 997 (2000).
32. R. Nageswara Rao, A. Narasa Raju and D. Nagaraju, An improved and validated LC method for resolution of bicalutamide enantiomers using amylose tris-(3,5-dimethylphenylcarbamate) as a chiral stationary phase, *J. Phar. Biomed. Anal.*, **42**, 347 (2006).
33. A. Berthod, W. Li and D.W. Armstrong, Multiple enantioselective retention mechanisms on derivatized cyclodextrin gas chromatographic chiral stationary phases, *Anal. Chem.*, **64**, 873 (1992).
34. B. Loun and D.S. Hage, Chiral separation mechanisms in protein-based HPLC columns. 1. Thermodynamic studies of (R)- and (S)-warfarin binding to immobilized human serum albumin, *Anal. Chem.*, **66**, 3814 (1994)
35. R.W. Stringham and J.A. Blackwell, Factors That Control Successful Entropically Driven Chiral Separations in SFC and HPLC, *Anal. Chem.*, **69**, 1414 (1997).